PAK4 Suppresses Motor Neuron Degeneration in hSOD1^{G93A} -Linked ALS Cell and Rat Models

Chaohua Cong
First Affiliated Hospital of Harbin Medical University
Weiwei Liang
First Affiliated Hospital of Harbin Medical University;Second Affiliated Hospital of Harbin Medical University
Chunting Zhang
First Affiliated Hospital of Harbin Medical University
Ying Wang
First Affiliated Hospital of Harbin Medical University
Yueqing Yang
Second Affiliated Hospital of Harbin Medical University
Xudong Wang
First Affiliated Hospital of Harbin Medical University
Shuyu Wang
First Affiliated Hospital of Harbin Medical University
Di Huo
First Affiliated Hospital of Harbin Medical University
Hongyong Wang
First Affiliated Hospital of Harbin Medical University
Di Wang
First Affiliated Hospital of Harbin Medical University
Honglin Feng (fenghonglin186@sina.com)
Harbin Medical College: Harbin Medical University https://orcid.org/0000-0002-5062-8846

Research

Keywords: PAK4, CREB pathway, degeneration, ALS

Posted Date: October 20th, 2020

DOI: https://doi.org/10.21203/rs.3.rs-93482/v1

Abstract

Background: Amyotrophic lateral sclerosis (ALS) is a fatal neurodegenerative disease characterized by the progressive loss of upper and lower motor neurons. The exact mechanisms underlying motor neuron death in ALS are still not fully understood, but a growing body of evidence indicates that inflammatory could accentuate disease severity and accelerate disease progression. Currently, no neuroprotective strategies have effectively prevented the progression of this disease.

Methods: IF, western blotting and RT-PCR were used to analyze the expression of PAK4 in vitro and in vivo models of ALS. We examined PAK4 function in ALS and the underlying mechanism by cell transfection, intraspinally injection of LV-PAK4 in hSOD1^{G93A} mice, flow cytometry, TUNEL staining, IF and western blotting.

Results: Here, we observed that the expression and activity of PAK4 significantly decreased in hSOD1^{G93A}-related cell and mouse models of ALS. In hSOD1^{G93A} mice the expression of PAK4 began to decrease at early-symptom stages of the disease. PAK4 silencing increased degeneration of motor neurons (NSC34 cells) and suppressed the CREB pathway. Overexpression of PAK4 protected motor neurons from hSOD1^{G93A}-induced degeneration by increasing the levels and transcriptional activity of CREB. The neuroprotective effect of PAK4 was markedly inhibited by compound 3i, a specific CREB inhibitor. In hSOD1^{G93A}-linked cell and mice, the CREB pathway, as the downstream target of decreased PAK4, was inhibited, and cell apoptosis increased. We also found that the expression of PAK4 was negatively regulated by miR-9-5p, and the miR-9-5p levels were upregulated in ALS. In vivo experiments revealed that PAK4 overexpression in the spinal neurons of hSOD1^{G93A} mice suppressed motor neuron degeneration, prolonged survival and promoted the CREB pathway.

Conclusion: These results indicate that PAK4 plays a protective role for motor neurons by targeting CREB, suggesting it may be a useful therapeutic target in ALS.

Introduction

Amyotrophic lateral sclerosis (ALS) is a heterogeneous, fatal neurodegenerative disorder characterized by progressive loss of motor neurons (MNs) in the brain, brainstem and spinal cord, resulting in motor and extra-motor symptoms [1–3]. Approximately 5–10% of patients with ALS are familial (fALS), most often in an autosomal dominant pattern [4, 5], whereas the rest of cases are sporadic (sALS) and may result from genetic mutations or environmental exposure [6]. Mutations in the SOD1 gene account for ~ 20% of fALS and ~ 5% of sALS [7, 8, 9], and transgenic mice carrying mutant SOD1 develop progressive paralysis [10]. Although the exact mechanisms underlying SOD1-induced toxicity are still mostly unknown [11], inflammation is proposed to cause MN degeneration in ALS. Currently, only riluzole and edaravone are approved by FDA for ALS clinical therapy. However, they could provide limited efficacy [12, 13]. Thus, strategies to promote MN survival remain an urgent need for ALS treatment.

CREB (cAMP-response-element binding protein) is a crucial transcription factor in the brain that regulates essential physiological functions including neuronal excitability, dendritic growth, long-term synaptic plasticity formation and neuronal survival [14–20]. CREB mediates neuroprotection mainly via its downstream genes, such as peroxisome proliferator- activated receptor gamma coactivator-1 alpha (PGC-1a) [21], brain-derived neurotrophic factor (BDNF) [22] and B-cell lymphoma 2 (Bcl-2) [23]. Deregulation of CREB signaling is associated with several neurodegenerative diseases, for instance, Alzheimer's disease (AD), Parkinson's disease (PD), Huntington's disease (HD) and ALS [22, 24–26]. Restoring CREB activity rescues defects in dendrite morphogenesis in TDP-43 misregulated neurons [27]. In particular, human adipose stem cell extract treatment improves MN function and prolongs the life span in ALS mice by increasing the expression of p-CREB [28]. Moreover, our group has demonstrated that the neuroprotective effect of lithium for ALS relies on attenuating the improper binding of mutant SOD1 protein aggregates with p-CREB [29]. Although CREB signal transduction networks are complex and obscure, it has been proved that the CREB pathway plays a neuroprotective role in ALS disease.

The serine/threonine p21-activated kinases (PAKs) are comprised of six mammalian proteins that are divided into group I (PAK1 to PAK3) and group II (PAK4 to PAK6) in terms of their structural and functional features [30]. Group II PAKs contribute to a wide range of intracellular processes including cytoskeletal dynamics, cell growth, tumorigenesis, neuronal dysfunction and cell survival [30–34]. Studies on PAK4 have revealed its pivotal role in cytoskeletal remodeling, neuronal development, axonal outgrowth and neuronal survival [24, 35, 36]. PAK4 knockout mice display dramatic defects in the heart and nervous system, with striking abnormalities observed in axonal outgrowth and neural tube formation [36]. Studies have shown that PAK4 expression in PD patients is down-regulated and that overexpressing it promotes DA neurons survival in the a-synuclein rat model [24]. Deregulation of AKT signaling is involved in ALS. Restoring AKT activation rescues MNs from death in ALS [37–40]. PAK4 is linked to AKT activity [41, 42]; thus, PAK4 may promote the survival of MNs through AKT. Together, these studies suggest that PAK4 plays a pivotal role in neuronal pathophysiology.

PAK4 has been shown to increase the levels and activity of CREB globally in diverse cell types [24, 43–45]. Given that PAK4 targets CREB and that CREB promotes MN survival, maintaining PAK4 activity is expected to play a pivotal role in preventing the progressive loss of MNs in ALS. Therefore, we hypothesized that decreased PAK4 activity might involve in the pathogenesis of ALS. We found that the expression and activity of PAK4 were deregulated in ALS models. Overexpression of PAK4 protected MNs from $hSOD1^{G93A}$- induced apoptosis, and this neuroprotective effect was alleviated by CREB inhibitor. Finally, $hSOD1^{G93A}$ mice injected with LV-PAK4 manifested a delay in disease onset, prolongation of survival and promotion of CREB signaling. These data suggest that the neuroprotective role of PAK4 in ALS MNs is mediated by the CREB pathway.

Methods

Animals

Transgenic mice carrying the hSOD1^{G93A} gene on the C57BL/6J strain background were obtained from Jackson Laboratory (Bar Harbor, ME, USA). All mice were bred and mainta- ined on a 12 h day/night cycle with adequate food and water. The offspring were identified by polymerase chain reaction (PCR) analysis of tail DNA [46]. Transgenic female mice were culled at postnatal day 75, 120 and 140, corresponding to presymptomatic, early-sym stage and late-sym stage of the disease. Age-matched non-transgenic female littermates were used as wild-type controls. All animal experiments were performed in accordance with the International Animal Care Guidelines and were approved by the Experimental Animal Ethics Committee of Harbin Medical University.

Generation of a hSOD1^{G93A}-transfected NSC34 cell line and cell cultures

The mouse neuroblastoma x spinal cord NSC34 cell line was a gift from Cedarlane Laboratories (Vancouver, Canada). NSC34 cells were stably transfected with hSOD1^{G93A}, human wild-type SOD1 or an empty lentivirus vector separately as described [47]. Puromycin at 200 μg/ml (G418, Invitrogen) was used to maintain a stable cell line translation. Cells were cultivated at 37ºC in a 5% CO_2-atmosphere in DMEM-supplemented 10% fetal bovine serum (FBS, Natocor) and 100 U/mL penicillin-streptomycin.

Immunohistochemistry and immunofluorescence staining

After anesthesia, the hSOD1^{G93A} and WT mice underwent transcardial perfusion with PBS, followed by perfusion with 4% PFA (paraformaldehyde) (PH = 7.4). The spinal cords were dissected and fixed in 4% PFA for 24 h, and then were embedded in paraffin. 3 μm sections of cervical or lumbar enlargements were prepared for immunohistochemistry and immunofluorescence staining. In brief, after deparaffinization and dehydration, sections were incubated with a primary antibody against PAK4 (1:200, Santa Cruz Biotechnology, sc- 390507) overnight at 4 °C. For the visualization, sections were incubated with secondary antibodies followed by DAB (3,3'-diaminobenzidine) staining. The images were captured using a Leica microscope (Leica, Wetzlar, Germany) and analyzed by Image-Pro Plus 6.0 software (Media Cybermetics, Inc., Silver Spring, MD, USA). For immunofluorescence staining, sections were incubated with primary antibody against PAK4 (1:150, Santa Cruz Biotechnology), anti-MAP-2 antibody (1:200, Beijing Bioss Biotechnology Co) and anti-cherry (1:500, Abcam) at 4 °C overnight. After washing, secondary anti-mouse/rabbit antibodies (1:200, ZSGB-BIO, Beijing) were used. Next, the sections were incubated with 4, 6-diamidino-2-phenylindole (DAPI) for 5 min at room temperature. The images were captured by an inverted fluorescence microscope (Zeiss Vert A1, Germany).

Immunofluorescence cytochemistry analysis

Cultured cells were washed three times with PBS and fixed for 20 min in 4% PFA (PH = 7.4) at room temperature. After being penetrated with 0.2% Triton X-100, cells were blocked with 5% BSA for 1 h. Then, the cells were incubated overnight at 4 °C with the primary antibodies (anti-PAK4, Santa Cruz Biotechnology) at 1:150 dilutions. Following 3 washes in PBS, cells were incubated with FITC-conjugated goat anti-mouse IgG (1:100) for 2 h at room temperature. After washing, cells were stained with DAPI

(Beyotime, Shanghai, China) for 3 min. An inverted fluorescence microscope (Zeiss Vert A1, Germany) was used for cell observation.

Western blotting analysis

The whole spinal cords from mice or prepared cells were lysed in RIPA lysis buffer (Beyotime Biotechnology Co.,Ltd., Shanghai, China) containing phosphatase and protease inhibitor mixture (Roche, 4906845001 and 04693132001). Lysates were centrifuged at 14000 RPM for 20 min at 4 °C, and only the supernatants were analyzed by western blotting, as described previously [47]. Primary antibodies: rabbit anti-PAK4 (1:1000, Cell Signaling Technology), rabbit anti-pPAK4 at Ser474 (1:1000, Cell Signaling Technology), rabbit anti-CREB (1:1000, Cell Signaling Technology), rabbit anti-pCREB at Ser133 (1:1000, Cell Signaling Technology), mouse anti-Bcl-2 monoclonal antibody (1:500, Bioss Antibodies), rabbit anti-PGC-1a (1:1000, Abcam), rabbit anti-total caspase-3 (1:2000, Abcam), rabbit anti-cleaved caspase-3 (1:500, Abcam), mouse anti-β-actin (1:1000, Beyotime). The blots were incubated with Alexa Fluor-800-conjugated secondary antibody (Goat anti-mouse or anti-rabbit, 1:10000, Li-COR) at room temperature for 1 h. For signal detection, an Odyssey infrared imaging system (Li-COR, USA) was used according to the manufacturer's instructions. The density of the blots was determined using Image J (http://imagej.nih.gov/ij/).

qRT-PCR

For PAK4 mRNA quantification, total RNA was extracted from spinal cords or prepared cells using Trizol (Cwbio); cDNA was generated using ReverTra Ace qPCR RT Master Mix with gDNA Remover (TOYOBO CO.,LTD. Life Science Department OSAKA JAPAN). For miR-9-5p detection, miRNA was collected with an miRNA Purification Kit (Cwbio) and then reverse-transcribed using an miRNA cDNA Synthesis Kit (Cwbio). qRT-PCR was performed on a Light Cycler 480 (Roche) using THUNDERBIRD SYBR qPCR Mix (TOYOBO CO.,LTD.Life Science Department OSAKA JAPAN) and an miRNA qPCR Assay Kit (Cwbio) according to the manufacturer's protocol. The following mouse primers were used: mPAK4, forward primer: 5'-GACTACCGGCACGAGAACG-3', reverse primer: 5'-CATCA TGGGTCAGCAAGATAGAG-3'; mβ-actin, forward primer: 5'-CCAGCCTTCCTTCTTGG GTAT-3', reverse primer: 5'-TGCTGGAAGGTGGACAGTGAG-3'; miR-9-5p, forward primer: 5'-ACACTCCAGCTGGGAGTATGTCGATCTATTG-3', reverse primer: 5'-TGGTGTCGTGGAGTCG-3'; U6, forward primer: 5'-CTCGCTTCGGCAGCACA-3', reverse primer: 5'-AACGCTTCACGAATTTGCGT-3'. The relative expression of PAK4 mRNA and miR-9-5p was analyzed using the $2^{-\Delta\Delta CT}$ method. qRT-PCR reactions were carried out in three independent runs in triplicate.

Oligonucleotide transfection

The siRNA sequences specific against mouse PAK4 (sense: 5'-GGAUGAACGAGGAA CAGAUTT-3', antisense: 5'-AUCUGUUCCUCGUUCAUCCTT-3') and non-targeting siRN- A control sequences (sense: 5'-UUCUCCGAACGUGUCACGUTT-3'; antisense: 5'-ACGU- GACACGUUCGGAGAATT-3') were obtained from Gene Pharma Co., Ltd (Shanghai, China). The miR-9-5p inhibitor and miR-NC were chemically synthesized by Gene Pharma. All transfections were carried out according to the manufacturer's protocols. Briefly, NSC34 cells were seeded in a 24-well format, and after reaching 70%-80% confluence, the siRNAs and

miRNA inhibitor were transfected into cells using Lipofectamine 2000 (Invitrogen). The effectiveness of transfection was evaluated by qRT-PCR and western blotting.

Plasmid transfection and treatment

The cDNA plasmid (OriGene, Beijing, China) mediated overexpression of PAK4 in mSOD1 cells was performed as previous description [48] using Lipofectamine 2000 (Invitrogen). mSOD1 cells transfected with p3xFlag-CMV-14 construct served as controls. At 48 h after transfection, cells containing cDNA or vehicle control were incubated with 50.26 ng/ml CREB inhibitor (compound 3i, Selleckchem, US). Then, mSOD1 cells were divided into four groups: 1) cDNA-PAK4 transfection group ($PAK4^+$); 2) empty-vector transfection group (EV); 3) empty-vector transfection plus the CREB inhibitor group (EV + 3i) and 4) cDNA-PAK4 transfection plus the CREB inhibitor group ($PAK4^+$+3i). All groups were incubated under standard growth conditions.

Cell apoptosis assay

To detect apoptosis, at 72 h after siPAK4 transfection or 3i treatment, cultures were subjected to flow cytometric analysis using an Annexin V-FITC/PI Kit (4A Biotech Co, Ltd) and TUNEL staining using an In Situ Cell Death Detection Kit (Roche, Basel, Switzerland). In brief, the prepared cells were stained with Annexin V-FITC for 5 min in the dark before being analyzed by flow cytometry. TUNEL staining was performed according to the manufacturer's instructions. The cells were incubated with TdT enzyme for 1 h at 37 °C in a humid chamber and then counter-stained with DAPI. The apoptosis index was determined by the number of TUNEL-positive/total number of nucleated cells × 100%.

Injections

The lentivirus vector that carried PAK4 cDNA (LV-PAK4) and the lentivirus control (LV-cherry) were purchased from the GenePharma Corporation (Shanghai, China). 60 days of age female $hSOD1^{G93A}$ mice were randomly divided into two groups: $hSOD1^{G93A}$/LV-PAK4 and $hSOD1^{G93A}$/LV-cherry groups (n = 15/group), and they were injected with LV-PAK4 or LV-cherry (6 ul, 2×10^8 TU/mL) into the mouse's L5 and L6 subarachnoid space using a glass micro-needle.

Disease course analysis and behavior tests

To test motor function, rotarod performance was examined in LV-PAK4 or LV-cherry injected $hSOD1^{G93A}$ mice starting at 80 days of age. After 1 week of training, each mouse was placed on the rotating rod at 16 rpm every 2 days to record the latency time before the mouse would fall off. The test was repeated three times for each animal. Disease onset was defined as the age at which a mouse could no longer stay on the rotating rod for 180 s. The date of disease endpoint was recorded when the mouse could not rise within 30 s after being placed on its side.

Statistical analyses

The data were analyzed using SPSS version 23.0 and GraphPad Prism 8.0 software (GraphPad Software, USA). Statistical significance was evaluated with Student's t-test or one-way analysis of variance

(ANOVA). Quantitative data were expressed as mean values of at least three determinations ± SD. Tests were considered statistically significant at $P < 0.05$.

Results

Reduced PAK4 expression and activity in the spinal cord of hSOD1^{G93A} mice

Immunofluorescence analyses of the spinal cords of hSOD1^{G93A} mice and age-matched non-transgenic littermates(WT) were performed to detect differences in PAK4 levels associated with ALS. Results showed that compared with WT, significantly reduced PAK4 (red) expression was observed in the MN (green) of hSOD1^{G93A} mice (Fig. 1A). Decreased PAK4 expression in ALS was confirmed by western blotting. We also found that the protein levels of pPAK4, an index of PAK4 activation, were lower in p140 hSOD1^{G93A} mice compared to WT (Fig. 1B and 1C). The pPAK4/PAK4 ratio was greater in hSOD1^{G93A} mice (Fig. 1D). These data suggested that the expression and activity of PAK4 in hSOD1^{G93A} mice were both down-regulated. Next, we analyzed PAK4 mRNA levels in the spinal cords of hSOD1^{G93A} mice (n = 6) and WT (n = 6) using qRT-PCR. It was found that the gene-expression pattern was followed by protein expression. The levels of PAK4 mRNA were significantly reduced in hSOD1^{G93A} mice (Fig. 1E).

To characterize the temporal expression patterns of PAK4 in ALS mice, we evaluated PAK4 levels in hSOD1^{G93A} and WT mice at three stages of the disease (the presymptomatic stage P75, early-sym stage P120 and late-sym stage P140) using immunohistochemistry. Results showed that in both groups, PAK4 was mainly expressed in the cytoplasm and nuclei of MN (Fig. 2A). Compared with WT, PAK4 immunoreactivity was significantly lower at early-sym and late-sym stages of the disease in ALS mice (Fig. 2A). However, at the presymptomatic stage, OD values of PAK4 were not significantly altered (Fig. 2B). Taking these data together, we predicted that PAK4 was involved in the pathophysiological process of ALS.

PAK4 protein levels and activity are down-regulated in mSOD1 cells

Next, we explored whether the expression and activity of PAK4 were altered in vitro models of ALS. NSC34 cells exhibit many MN characteristics, including the generation of action potentials, expression of neurofilament proteins and synthesis of acetylcholine [49–51]. Our group has confirmed that choline acetyltransferase, an MN marker, is expressed in NSC34 cells [40]. Thus, NSC34 cells stably transfected with hSOD1^{G93A} (mSOD1) were used as a cell model of ALS in subsequent studies. Immunocytochemistry staining showed that PAK4 (red) was expressed both in the cytoplasm and nuclei of pLV, wtSOD1 and mSOD1 cells. Compared to pLV cells, mSOD1 cells displayed weaker fluorescence intensity of PAK4, while wtSOD1 cells displayed a similar intensity (Fig. 3A). Decreased PAK4 expression in mSOD1 cells was confirmed by western blotting. We also found that compared with pLV, protein levels

of pPAK4 were significantly decreased in mSOD1 cells, while wtSOD1 and pLV cells had similar pPAK4 protein levels (Fig. 3B and 3C). The pPAK4/PAK4 ratio in mSOD1 cells was greater than in control pLV and wtSOD1 cells (Fig. 3D). These data suggested that the expression and activity of PAK4 in mSOD1 were both down-regulated. Next, qRT-PCR analysis suggested that PAK4 mRNA levels of mSOD1 cells were robustly downregulated to approximately 18.9% compared to pLV cells. PAK4 mRNA expression in wtSOD1 and pLV cells showed no statistical difference (Fig. 3E).

Knockdown of PAK4 promotes motor neuron degeneration and decreases the levels and activity of CREB

To determine the biological role of PAK4 in MN, we selected NSC34 cells with many MN characteristics for further study. Three siRNAs targeting PAK4 were transfected into NSC34 cells, and the efficiency of PAK4 knockdown was evaluated by western blotting and qRT-PCR (Fig. 4A). We selected siPAK4-2 for subsequent experiments because of its obvious knockdown effects. Flow cytometry analysis suggested that NSC34 cells transfected with siPAK4-2 yielded a significantly higher rate of cell apoptotic death (49.34 ± 0.95%) than siNC control (32.07 ± 2.45%) (Fig. 4B and Fig. 4C). Consistently, TdT-mediated dUTP nick end labeling (TUNEL) staining indicated that knockdown of PAK4 significantly increased the percentage of cells experiencing apoptotic death (35.67 ± 2.51%), and in the siNC group, the percentage of cell apoptosis was 20.57 ± 1.50% (Fig. 4D and Fig. 4E). These data suggested that PAK4 protected NSC34 cells from apoptotic death.

Next, we further investigated the mechanism by which PAK4 promoted cell survival. Previous studies have revealed that PAK4 is a critical regulator of CREB and that CREB promotes MN survival [52]. Thus, western blotting of PAK4, CREB, pCREB and the CREB target proteins (PGC-1a and Bcl-2) was performed with extract from siNC and siPAK4-2 groups. The results showed that the levels of CREB, pCREB, Bcl-2 and PGC-1a were decreased in PAK4 knockdown NSC34 cells. These data indicated that PAK4 might inhibit motor neuron degeneration via the CREB pathway (Fig. 4F and 4G).

CREB pathway mediates PAK4-induced neuroprotection in mSOD1 cells

To investigate whether the neuroprotective role of PAK4 would extend to cell models of ALS, we upregulated PAK4 expression using a plasmid vector for PAK4 in mSOD1 cells. The results of western blotting and qRT-PCR showed that PAK4 plasmid significantly increased PAK4 expression in mSOD1 cells (Fig. 5A). To further determine whether the possible neuroprotective effect of PAK4 in mSOD1 cells was mediated by CREB signaling, we selectively inhibited CREB function by using compound 3i (a specific inhibitor of CREB) while transfecting the PAK4 plasmid or empty-vector (EV). Accordingly, the results showed that the percentage of cell apoptotic death was lowest in the $PAK4^{+}$ group (15.19 ± 1.98%). In the $PAK4^{+}$+3i group, 3i impaired the neuroprotective function of PAK4 (24.93 ± 2.27%). In the EV and EV + 3i groups, the percentages of apoptotic death were 31.70 ± 1.68% and 45.70 ± 0.87% (Fig. 5B and 5C). This effect was further confirmed by TUNEL (Fig. 5D and 5E), and administration of PAK4 improved mSOD1 cell viability (10.25 ± 1.29%). The ability of PAK4 to relieve mSOD1-induced cytotoxicity was

compromised in the PAK4^{+}+3i group (16.28 ± 0.86%). In the EV and EV + 3i groups, the percentages of apoptotic death were 20.84 ± 2.17% and 34.39 ± 1.89%. Furthermore, western blotting studies confirmed increased PAK4, CREB, pCREB, Bcl-2 and PGC-1a levels in the PAK4^{+} group compared with EV control (Fig. 6A-F). In addition, 3i inhibited CREB phosphorylation and transcription activity effectively. Compared with the PAK4^{+} group, the levels of pCREB, Bcl-2 and PGC-1a were decreased in the PAK4^{+}+3i group, while the levels of PAK4 and CREB showed no significant changes (Fig. 6A, 6E-F). Thus, these data suggested that CREB and its target proteins BCL-2, PGC-1a mediated the neuroprotective effect of PAK4.

CREB pathway and motor neuron survival are suppressed in mSOD1 cells and hSOD1^{G93A} mice

To explore the effects of deregulated PAK4 expression on downstream consequences and neurodegeneration in ALS models, the protein levels of CREB signaling and cleaved-caspase3 were analyzed in mSOD1 cells and the spinal cords from hSOD1^{G93A} mice. Immunoblotting analysis revealed that mSOD1 cells exhibited low levels of CREB, pCREB and CREB target proteins than pLV cells, while wtSOD1 cells displayed similar levels (Fig. 7A and 7B). Down-regulated PAK4 markedly increased the levels of cleaved-caspase3 in mSOD1 cells (Fig. 7A and 7C). In the in vivo study, the levels of CREB, pCREB, Bcl-2 and PGC-1a in the spinal cords of late-sym stage hSOD1^{G93A} mice were significantly reduced compared with WT (Fig. 7D and 7E). Moreover, hSOD1^{G93A} mice exhibited higher levels of cleaved-caspase3 than control (Fig. 7D and 7F). These data suggested that down-regulated PAK4 expression impaired the CREB pathway and promoted neurodegeneration in ALS models.

PAK4 expression is negatively regulated by miR-9-5p in ALS

MicroRNAs (miRNAs), small non-coding RNAs, repress gene translation and promote target mRNA degradation [53]. It has been reported that PAK4 is target regulated by a variety of miRNAs, including miR-433 [54], miR-224 [55], miR-199a-3p [56] and miR-9-5p [57]. Moreover, the expression of miR-9-5p in the cerebrospinal fluid of ALS patients is increased [58]. We speculated that PAK4 might be inversely regulated by miR-9-5p in ALS. To test our hypothesis, we first analyzed miR-9-5p levels in ALS models using qRT-PCR. Results showed that compared with control, the expression of miR-9-5p in spinal cords of p140 hSOD1^{G93A} mice was increased, especially in the mSOD1 cell line (Fig. 8A). In our previous studies, we have found that the mRNA levels of PAK4 were decreased in vivo and in vitro models of ALS (Fig. 1E and 3D). To determine whether miR-9-5p negatively regulated PAK4 mRNA expression, miR-9-5p inhibitor transfection was conducted on mSOD1 cells. The results showed that downregulation of miR-9-5p significantly upregulated the expression of PAK4 mRNA and protein (Fig. 8B).

Delayed disease onset and extended lifespan of hSOD1^{G93A} mice injected with LV-PAK4

Since PAK4 played a neuroprotective role in vitro, we next evaluated the in vivo biological function in hSOD1^{G93A} mice. We injected hSOD1^{G93A} mice intraspinally at 60 days of age with LV-PAK4 or LV-cherry. Four weeks postinjection, the spinal cord sections of treated mice were examined for cherry expression by immunofluorescence (Fig. 9A). The data showed that transduction efficiency was high in the ventral horns of the lumbar spinal cord. Western blotting and qRT-PCR further determined the results. The protein levels of PAK4 were higher in the spinal cords of LV-PAK4-injected mice compared with LV-cherry-injected ones (Fig. 9B). Furthermore, qRT-PCR detected significantly higher PAK4 mRNA levels in LV-PAK4 injected mice compared with the controls (Fig. 9C).

Disease onset (measured by the rotarod test) was significantly delayed by a median of 16 d for hSOD1^{G93A} mice injected with LV-PAK4 compared with the hSOD1^{G93A} littermates injected with LV-cherry (LV-PAK4:124 d; LV-cherry:108 d; $P < 0.01$) (Fig. 9D). Moreover, survival of the LV-PAK4-injected hSOD1^{G93A} mice was remarkably extended, yielding a median survival time of 21 d beyond that of the LV-cherry-injected ones (LV-PAK4:157 d; LV-cherry:136 d; $P < 0.01$) (Fig. 9E). The LV-PAK4 treated mice had increased disease duration (the time from disease onset to endpoint), indicating slower disease progression, compared with the LV-cherry injected mice (LV-cherry: 28 d; LV-PAK4: 35 d; $P < 0.05$) (Fig. 9F).

Overexpression of PAK4 protects motor neurons from degeneration and enhances CREB signaling in hSOD1^{G93A} mice

To test the effects of PAK4 overexpression on MN degeneration, we performed immunostaining with anti-MAP-2 to examine the number of MNs in the spinal cords of LV treated hSOD1^{G93A} mice. We found that the number of MNs surviving in LV-PAK4-injected mice was significantly increased compared with LV-cherry-injected mice (cervical spinal cord: 32.00 ± 3.61 vs. 12.33 ± 2.08; lumbar spinal cord: 29.67 ± 3.06 vs. 14.33 ± 2.52; $P < 0.05$) (Fig. 10A and 10B). Furthermore, immunoblotting analysis was performed to determine the effects of PAK4 overexpression on downstream consequences and neurodegeneration. Results revealed that LV-PAK4 injected mice exhibited low levels of CREB, pCREB, PGC-1a and Bcl-2 compared with LV-cherry injected mice (Fig. 10C and 10D). Overexpression of PAK4 markedly decreased the levels of cleaved-caspase3 in hSOD^{1G93A} mice (Fig. 10C and 10E). These data suggested that PAK4 exerted neuroprotective effects by activating CREB signaling in the hSOD1^{G93A} mouse models of ALS.

Discussion

ALS is a relentless and fatal neurodegenerative disease. Development of neuroprotective treatments to prevent or delay the progression of the disease remains an unachieved goal. Here, we validate for the first time that PAK4 is a crucial survival factor for MN. The expression and activity of PAK4 are downregulated in vivo and in vitro models of ALS. Activation or overexpression of PAK4 and its downstream signaling pathways might serve as a new potential therapeutic method for ALS.

PAK4 expresses ubiquitously and plays an essential role in multiple biological processes [36, 59]. Dysregulation of PAK4 expression involves in various diseases [60]. The functions of PAK4 in diseases have principally been investigated in cancers, and overexpression of it contributes to tumorigenesis [61–63]. In the nervous system, PAK4 is required for neuronal development and axonal outgrowth [35, 36]. In dopaminergic neurons of PD patients, the expression and activity of PAK4 are down-regulated and this decline may promote PD pathogenesis [24]. However, the relationship between PAK4 and ALS disease remains unclear. In this context, we demonstrate for the first time that PAK4 protein expression as well as activity significantly declined in cells and mice carrying $hSOD1^{G93A}$. Considering that the expression of PAK4 declined at early-sym stages, PAK4 might be involved in ALS disease progression.

A series of findings have shown that activated CREB promotes neuronal survival through a transcription-dependent pathway [14–17, 20]. Moreover, the activation of CREB- mediated downstream proteins plays a neuroprotective role in PD and AD rat models [22, 24, 64]. Increasing expression of p-CREB can improve MN function and prolong the life span of ALS mice [28]. In accordance with previous studies, we found that PAK4 protected MN from mSOD1-induced cytotoxicity through increasing CREB expression and activity. 3i amelior- ated the neuroprotective effects of PAK4 and increased apoptosis by inhibiting the transcription activity and phosphorylation of CREB in ALS cell models. Thus, we further confirmed the protective role of CREB in the normal nervous system and neurodegenerative diseases.

Accumulating evidence suggests that CREB is a target of PAK4. In the present study, we found that knockdown of PAK4 reduced the levels and activity of CREB in NSC34 cells. Overexpression of PAK4 increased CREB levels and activity in mSOD1 cells. In mice and cell models of ALS, the low expression of PAK4 caused inhibition of the CREB pathway and promoted MN degeneration. Cumulatively, our findings are consistent with previous works that PAK4 sustains high CREB levels and improves CREB activity in various tissues [43, 44]. However, it is unclear how PAK4 maintains high levels of CREB. Additional studies are required to further elucidate the relationship between PAK4 and CREB expression and degradation. PAK4 could not directly phosphorylate CREB in vitro, suggesting that PAK4 activated CREB transcription by maintaining a high level. Whether PAK4 increases the transcriptional activity of CREB through a phosphorylation-independent pathway in ALS needs subsequent study.

Growing evidence reveals that mitochondrial dysfunction plays a crucial role in ALS [65]. PAK4 can inactivate the pro-apoptotic protein BAD (members of the Bcl-2 family pro- apoptotic activities) by specifically phosphorylating S112 [66]. This phosphorylation protects cells from apoptosis by inhibiting BAD localization in the mitochondrial outer membrane. siRNA treatment decreased PAK4 expression in parallel with inhibition of the CREB downstream effector proteins PGC-1a and Bcl-2. Conversely, overexpression of PAK4 promoted the levels of Bcl-2 and PGC-1a in cell models of ALS. Moreover, 3i decreased PAK4-induced expression of the CREB downstream proteins Bcl-2 and PGC-1a, thereby reducing cell survival. These data demonstrate that the up-regulation of Bcl-2 and PGC-1a mediates PAK4-induced neuroprotection. Considering the close association of PGC-1a and Bcl-2 with mitochondrial health [67, 68], PAK4 may contribute to mitochondrial protection in a transcription-dependent manner.

Thus, transcription-dependent and transcription- independent theories could explain the mechanisms that PAK4 protects mitochondria in the presence of neurotoxic stimuli.

Although PAK4 is a potential therapeutic target for ALS, persistent expression of it in the spinal cord after gene therapy might contribute to tumorigenesis because PAK4 is a potent oncogene. However, we did not monitor tumor formation in LV-PAK4 injected hSOD1^{G93A} mice, but we did not maintain lengthy follow-up. In addition, a lower cancer risk was observed in human ALS patients after diagnosis compared with healthy individuals [69]. Thus, we speculate that a lack of tumorigenesis is likely due to a poor microenvironment for cell survival and proliferation in neurodegenerative diseases. ALS is characterized by progressive death of upper and lower MN, suggesting that the brain and spinal cord could not provide a proliferative environment. Moreover, most primary brain tumors develop from glial and meningeal cells. Thus, although PAK4 is regarded as an oncogenic gene, if a local delivery method can guarantee MN-specific targeting, this could prevent undesirable effects and provide a promising therapeutic intervention for ALS. We also consider CREB as another target for modulation of the PAK4 neuroprotective pathway. CREB may be less potent than PAK4 because the role of CREB is more restricted compared with PAK4, but it may specifically enhance the expression of Bcl-2 with a reduced risk of tumor formation.

Group I of the PAK proteins plays a vital role in spinocerebellar ataxia type 1 (SCA1) [52], fragile X syndrome (FXS) [70], X-linked mental retardation [71], and neurodegenerative diseases such as HD [31, 32] and AD [72]. Rescue from disease pathology in cell and mice models of SCA1 and improvement of abnormal behavior in FXS mice model by group I PAK inhibitors, offer proof of PAKs as therapeutic targets [73, 74]. Recent studies have implicated PAK4 and PAK6 in PD by demonstrating that PAK4 plays a neuroprotective role in PD models and that PAK6 is a downstream regulator of PD-causing mutations [24, 75]. Moreover, PAK signaling is stimulated by ALS2; mutations in the ALS2 gene cause some rare juvenile forms of ALS [76, 77]. Our findings demonstrated that PAK4 plays a neuroprotective role in ALS models. In aggregate, these studies suggest that dysregulation of PAKs is a pathogenic mechanism in a series of neurological diseases. Thus, the development of more selective and effective interventions targeting PAKs may be a promising therapeutic strategy.

In summary, the current findings identify a neuroprotective role for PAK4 in ALS models. A limitation of this study is the absence of human postmortem brain samples; accordingly, we did not study how PAK4 expression levels correlate with ALS in human patients. Further work needs to address the mechanism for PAK4 increasing the levels of CREB and determine if there are other mechanisms for PAK4 enhancing CREB transcriptional activity in ALS. The neuroprotective pathway of PAK4 still needs to be better clarified before targeting PAK4 as a therapeutic strategy in patients with ALS.

Conclusions

This work demonstrates that PAK4 protein levels and activity are down-regulated in hSOD1^{G93A}-linked ALS cell and rat models, and overexpression of it protects motor neurons from degeneration. The

neuroprotective effect of PAK4 is mediated by activation of CREB sianaling pathway. Therefore, PAK4 may be a potential therapeutic target in ALS.

Abbreviations

Amyotrophic lateral sclerosis (ALS); p21-Activated kinase 4 (PAK4); cAMP-response element binding protein (CREB); Cu-Zn superoxide dismutase (SOD1); TAR DNA-binding protein (TDP-43); microtubule associated protein-2 (MAP-2); peroxisome proliferator-activated receptor gamma coactivator-1 alpha (PGC-1a); B cell lymphoma 2 (Bcl-2); brain-derived neurotrophic factor (BDNF); motor neuron (MN)

Declarations

Acknowledgements

We are very grateful to Dr. Shengwang Liu from the Harbin Veterinary Research Institute, Chinese Academy of Agricultural Sciences and Dr. Yu Chen from the Brain Cognition and Brain Disease Institute, Shenzhen Institutes of Advanced Technology , Chinese Academy of Sciences for the assistance with our work. .

Authors'contributions

Chaohua Cong, Weiwei Liang and Chunting Zhang conceived and designed the study. Chaohua Cong and Ying Wang conducted the experiments. Yueqing Yang, Xudong Wang and Shuyu Wang analyzed the data, and drafted the manuscript. Di Huo, Hongyong Wang and Di Wang participated in writing the manuscript. The authors read and approved the final manuscript.

Funding

This work was supported by grants from the National Nature Science Foundation of China (No. 91849133 and No. 81571227), as well as the Innovative research program for graduates of Harbin Medical University (No. YJSKYCX2018-32HYD).

Availability of data and materials

The datasets used during the current study are available from the corresponding author on reasonable request.

Ethics approval

All animal experiments were performed in accordance with the International Animal Care Guidelines and were approved by the Experimental Animal Ethics Committee of Harbin Medical University.

Consent for publication

Not applicable.

Competing interests

The authors declare that they have no competing interests.

References

1. Zufiría M, Gil-Bea FJ, Fernández-Torrón R, et al. ALS: A bucket of genes, environment, metabolism and unknown ingredients. Prog Neurobiol. 2016;142:104-129.
2. Hardiman O, Al-Chalabi A, Chio A, et al. Amyotrophic lateral sclerosis [published correction appears in Nat Rev Dis Primers. 2017 Oct 20;3:17085].
3. Clerc P, Lipnick S, Willett C. A look into the future of ALS research. Drug Discov Today. 2016;21(6):939-949.
4. Sreedharan J, Blair IP, Tripathi VB, et al. TDP-43 mutations in familial and sporadic amyotrophic lateral sclerosis. Science. 2008;319(5870):1668-1672.
5. Byrne S, Walsh C, Lynch C, et al. Rate of familial amyotrophic lateral sclerosis: a systematic review and meta-analysis. J Neurol Neurosurg Psychiatry. 2011;82(6):623-627.
6. Renton AE, Chiò A, Traynor BJ. State of play in amyotrophic lateral sclerosis genetics. Nat Neurosci. 2014;17(1):17-23.
7. Andersen PM, Al-Chalabi A. Clinical genetics of amyotrophic lateral sclerosis: what do we really know?. Nat Rev Neurol. 2011;7(11):603-615.
8. Majoor-Krakauer D, Willems PJ, Hofman A. Genetic epidemiology of amyotrophic lateral sclerosis. Clin Genet. 2003;63(2):83-101.
9. Robberecht W, Philips T. The changing scene of amyotrophic lateral sclerosis. Nat Rev Neurosci. 2013;14(4):248-264.
10. Gurney ME, Pu H, Chiu AY, et al. Motor neuron degeneration in mice that express a human Cu,Zn superoxide dismutase mutation [published correction appears in Science 1995 Jul 14;269(5221):149]. Science. 1994;264(5166):1772-1775.
11. Rothstein JD. Current hypotheses for the underlying biology of amyotrophic lateral sclerosis. Ann Neurol. 2009;65 Suppl 1:S3-S9.
12. Bensimon G, Lacomblez L, Meininger V. A controlled trial of riluzole in amyotrophic lateral sclerosis. ALS/Riluzole Study Group. N Engl J Med. 1994;330(9):585-591.
13. Yoshino H, Kimura A. Investigation of the therapeutic effects of edaravone, a free radical scavenger, on amyotrophic lateral sclerosis (Phase II study). Amyotroph Lateral Scler. 2006;7(4):241-245.
14. Zhou Y, Won J, Karlsson MG, et al. CREB regulates excitability and the allocation of memory to subsets of neurons in the amygdala. Nat Neurosci. 2009;12(11):1438-1443.

15. Dong Y, Green T, Saal D, et al. CREB modulates excitability of nucleus accumbens neurons. Nat Neurosci. 2006;9(4):475-477.
16. Lopez de Armentia M, Jancic D, Olivares R, Alarcon JM, Kandel ER, Barco A. cAMP response element-binding protein-mediated gene expression increases the intrinsic excitability of CA1 pyramidal neurons. J Neurosci. 2007;27(50):13909-13918.
17. Sargin D, Mercaldo V, Yiu AP, et al. CREB regulates spine density of lateral amygdala neurons: implications for memory allocation. Front Behav Neurosci. 2013;7:209. Published 2013 Dec 20.
18. Lonze BE, Riccio A, Cohen S, Ginty DD. Apoptosis, axonal growth defects, and degeneration of peripheral neurons in mice lacking CREB. Neuron. 2002;34(3):371-385.
19. Li S, Zhang C, Takemori H, Zhou Y, Xiong ZQ. TORC1 regulates activity-dependent CREB-target gene transcription and dendritic growth of developing cortical neurons. J Neurosci. 2009;29(8):2334-2343.
20. Viosca J, Lopez de Armentia M, Jancic D, Barco A. Enhanced CREB-dependent gene expression increases the excitability of neurons in the basal amygdala and primes the consolidation of contextual and cued fear memory. Learn Mem. 2009;16(3):193-197.
21. Chaturvedi RK, Hennessey T, Johri A, et al. Transducer of regulated CREB-binding proteins (TORCs) transcription and function is impaired in Huntington's disease. Hum Mol Genet. 2012;21(15):3474-3488.
22. Jeong H, Cohen DE, Cui L, et al. Sirt1 mediates neuroprotection from mutant huntingtin by activation of the TORC1 and CREB transcriptional pathway. Nat Med. 2011;18(1):159-165.
23. Mabuchi T, Kitagawa K, Kuwabara K, et al. Phosphorylation of cAMP response element-binding protein in hippocampal neurons as a protective response after exposure to glutamate in vitro and ischemia in vivo. J Neurosci. 2001;21(23):9204-9213.
24. Won SY, Park MH, You ST, et al. Nigral dopaminergic PAK4 prevents neurodegeneration in rat models of Parkinson's disease. Sci Transl Med. 2016;8(367):367ra170.
25. Yamashita M, Nonaka T, Hirai S, et al. Distinct pathways leading to TDP-43-induced cellular dysfunctions. Hum Mol Genet. 2014;23(16):4345-4356.
26. España J, Valero J, Miñano-Molina AJ, et al. beta-Amyloid disrupts activity-dependent gene transcription required for memory through the CREB coactivator CRTC1. J Neurosci. 2010;30(28):9402-9410.
27. Herzog JJ, Xu W, Deshpande M, et al. TDP-43 dysfunction restricts dendritic complexity by inhibiting CREB activation and altering gene expression. Proc Natl Acad Sci U S A. 2020;117(21):11760-11769.
28. Jeon GS, Im W, Shim YM, et al. Neuroprotective Effect of Human Adipose Stem Cell-Derived Extract in Amyotrophic Lateral Sclerosis. Neurochem Res. 2016;41(4):913-923.
29. Yin X, Wang S, Wang X, et al. Lithium facilitates removal of misfolded proteins and attenuated faulty interaction between mutant SOD1 and p-CREB (Ser133) through enhanced autophagy in mutant hSOD1G93A transfected neuronal cell lines. Mol Biol Rep. 2019;46(6):6299-6309.
30. Arias-Romero LE, Chernoff J. A tale of two Paks. Biol Cell. 2008;100(2):97-108.

31. Luo S, Mizuta H, Rubinsztein DC. p21-activated kinase 1 promotes soluble mutant huntingtin self-interaction and enhances toxicity. Hum Mol Genet. 2008;17(6):895-905.
32. Ma QL, Yang F, Frautschy SA, Cole GM. PAK in Alzheimer disease, Huntington disease and X-linked mental retardation. Cell Logist. 2012;2(2):117-125.
33. Kreis P, Thévenot E, Rousseau V, Boda B, Muller D, Barnier JV. The p21-activated kinase 3 implicated in mental retardation regulates spine morphogenesis through a Cdc42-dependent pathway. J Biol Chem. 2007;282(29):21497-21506.
34. Nekrasova T, Jobes ML, Ting JH, Wagner GC, Minden A. Targeted disruption of the Pak5 and Pak6 genes in mice leads to deficits in learning and locomotion. Dev Biol. 2008;322(1):95-108.
35. Dan C, Nath N, Liberto M, Minden A. PAK5, a new brain-specific kinase, promotes neurite outgrowth in N1E-115 cells. Mol Cell Biol. 2002;22(2):567-577.
36. Qu J, Li X, Novitch BG, et al. PAK4 kinase is essential for embryonic viability and for proper neuronal development. Mol Cell Biol. 2003;23(20):7122-7133.
37. Mitra J, Hegde PM, Hegde ML. Loss of endosomal recycling factor RAB11 coupled with complex regulation of MAPK/ERK/AKT signaling in postmortem spinal cord specimens of sporadic amyotrophic lateral sclerosis patients. Mol Brain. 2019;12(1):55.
38. Tan H, Chen M, Pang D, et al. LanCL1 promotes motor neuron survival and extends the lifespan of amyotrophic lateral sclerosis mice. Cell Death Differ. 2020;27(4):1369-1382.
39. Kirby J, Ning K, Ferraiuolo L, et al. Phosphatase and tensin homologue/protein kinase B pathway linked to motor neuron survival in human superoxide dismutase 1-related amyotrophic lateral sclerosis. Brain. 2011;134(Pt 2):506-517.
40. Zhang C, Yang Y, Liang W, et al. Neuroprotection by urate on the mutant hSOD1-related cellular and Drosophila models of amyotrophic lateral sclerosis: Implication for GSH synthesis via activating Akt/GSK3β/Nrf2/GCLC pathways. Brain Res Bull. 2019;146:287-301.
41. Tyagi N, Bhardwaj A, Singh AP, McClellan S, Carter JE, Singh S. p-21 activated kinase 4 promotes proliferation and survival of pancreatic cancer cells through AKT- and ERK-dependent activation of NF-κB pathway. Oncotarget. 2014;5(18):8778-8789.
42. Kuijl C, Savage ND, Marsman M, et al. Intracellular bacterial growth is controlled by a kinase network around PKB/AKT1. Nature. 2007;450(7170):725-730.
43. Park MH, Lee HS, Lee CS, et al. p21-Activated kinase 4 promotes prostate cancer progression through CREB. Oncogene. 2013;32(19):2475-2482.
44. Yun CY, You ST, Kim JH, et al. p21-activated kinase 4 critically regulates melanogenesis via activation of the CREB/MITF and β-catenin/MITF pathways. J Invest Dermatol. 2015;135(5):1385-1394.
45. Ryu BJ, Lee H, Kim SH, et al. PF-3758309, p21-activated kinase 4 inhibitor, suppresses migration and invasion of A549 human lung cancer cells via regulation of CREB, NF-κB, and β-catenin signalings. Mol Cell Biochem. 2014;389(1-2):69-77.

46. Feng HL, Leng Y, Ma CH, Zhang J, Ren M, Chuang DM. Combined lithium and valproate treatment delays disease onset, reduces neurological deficits and prolongs survival in an amyotrophic lateral sclerosis mouse model. Neuroscience. 2008;155(3):567-572.
47. Yin X, Ren M, Jiang H, et al. Downregulated AEG-1 together with inhibited PI3K/Akt pathway is associated with reduced viability of motor neurons in an ALS model. Mol Cell Neurosci. 2015;68:303-313.
48. Yang YQ, Zheng YH, Zhang CT, et al. Wild-type p53-induced phosphatase 1 down-regulation promotes apoptosis by activating the DNA damage-response pathway in amyotrophic lateral sclerosis. Neurobiol Dis. 2020;134:104648.
49. Hunter DD, Cashman N, Morris-Valero R, Bulock JW, Adams SP, Sanes JR. An LRE (leucine-arginine-glutamate)-dependent mechanism for adhesion of neurons to S-laminin. J Neurosci. 1991;11(12):3960-3971.
50. Cashman NR, Durham HD, Blusztajn JK, et al. Neuroblastoma x spinal cord (NSC) hybrid cell lines resemble developing motor neurons. Dev Dyn. 1992;194(3):209-221.
51. Durham HD, Dahrouge S, Cashman NR. Evaluation of the spinal cord neuron X neuroblastoma hybrid cell line NSC-34 as a model for neurotoxicity testing. Neurotoxicology. 1993;14(4):387-395.
52. Park J, Al-Ramahi I, Tan Q, et al. RAS-MAPK-MSK1 pathway modulates ataxin 1 protein levels and toxicity in SCA1. Nature. 2013;498(7454):325-331.
53. Rupaimoole R, Calin GA, Lopez-Berestein G, Sood AK. miRNA Deregulation in Cancer Cells and the Tumor Microenvironment. Cancer Discov. 2016;6(3):235-246.
54. Xue J, Chen LZ, Li ZZ, Hu YY, Yan SP, Liu LY. MicroRNA-433 inhibits cell proliferation in hepatocellular carcinoma by targeting p21 activated kinase (PAK4). Mol Cell Biochem. 2015;399(1-2):77-86.
55. Xia M, Wei J, Tong K. MiR-224 promotes proliferation and migration of gastric cancer cells through targeting PAK4. Pharmazie. 2016;71(8):460-464.
56. Zeng B, Shi W, Tan G. MiR-199a/b-3p inhibits gastric cancer cell proliferation via down-regulating PAK4/MEK/ERK signaling pathway. BMC Cancer. 2018;18(1):34. Published 2018 Jan 5.
57. Wang M, Gao Q, Chen Y, Li Z, Yue L, Cao Y. PAK4, a target of miR-9-5p, promotes cell proliferation and inhibits apoptosis in colorectal cancer. Cell Mol Biol Lett. 2019;24:58. Published 2019 Nov 8.
58. Waller R, Wyles M, Heath PR, et al. Small RNA Sequencing of Sporadic Amyotrophic Lateral Sclerosis Cerebrospinal Fluid Reveals Differentially Expressed miRNAs Related to Neural and Glial Activity. Front Neurosci. 2018;11:731. Published 2018 Jan 9.
59. Abo A, Qu J, Cammarano MS, et al. PAK4, a novel effector for Cdc42Hs, is implicated in the reorganization of the actin cytoskeleton and in the formation of filopodia. EMBO J. 1998;17(22):6527-6540.
60. Won SY, Park JJ, Shin EY, Kim EG. PAK4 signaling in health and disease: defining the PAK4-CREB axis. Exp Mol Med. 2019;51(2):1-9.

61. Radu M, Semenova G, Kosoff R, Chernoff J. PAK signalling during the development and progression of cancer. Nat Rev Cancer. 2014;14(1):13-25.
62. Fulciniti M, Martinez-Lopez J, Senapedis W, et al. Functional role and therapeutic targeting of p21-activated kinase 4 in multiple myeloma. Blood. 2017;129(16):2233-2245.
63. Costa TDF, Zhuang T, Lorent J, et al. PAK4 suppresses RELB to prevent senescence-like growth arrest in breast cancer. Nat Commun. 2019;10(1):3589. Published 2019 Aug 9.
64. Chang YM, Ashok Kumar K, Ju DT, et al. Dipeptide IF prevents the effects of hypertension-induced Alzheimer's disease on long-term memory in the cortex of spontaneously hypertensive rats. Environ Toxicol. 2020;35(5):570-581.
65. Choi SY, Lopez-Gonzalez R, Krishnan G, et al. C9ORF72-ALS/FTD-associated poly(GR) binds Atp5a1 and compromises mitochondrial function in vivo. Nat Neurosci. 2019;22(6):851-862.
66. Gnesutta N, Qu J, Minden A. The serine/threonine kinase PAK4 prevents caspase activation and protects cells from apoptosis. J Biol Chem. 2001;276(17):14414-14419.
67. Shin JH, Ko HS, Kang H, et al. PARIS (ZNF746) repression of PGC-1α contributes to neurodegeneration in Parkinson's disease. Cell. 2011;144(5):689-702.
68. Yuan J, Yankner BA. Apoptosis in the nervous system. Nature. 2000;407(6805):802-809.
69. Fang F, Al-Chalabi A, Ronnevi LO, et al. Amyotrophic lateral sclerosis and cancer: a register-based study in Sweden. Amyotroph Lateral Scler Frontotemporal Degener. 2013;14(5-6):362-368.
70. Hayashi ML, Rao BS, Seo JS, et al. Inhibition of p21-activated kinase rescues symptoms of fragile X syndrome in mice. Proc Natl Acad Sci U S A. 2007;104(27):11489-11494.
71. Allen KM, Gleeson JG, Bagrodia S, et al. PAK3 mutation in nonsyndromic X-linked mental retardation. Nat Genet. 1998;20(1):25-30.
72. Zhao L, Ma QL, Calon F, et al. Role of p21-activated kinase pathway defects in the cognitive deficits of Alzheimer disease. Nat Neurosci. 2006;9(2):234-242.
73. Bondar VV, Adamski CJ, Onur TS, et al. PAK1 regulates ATXN1 levels providing an opportunity to modify its toxicity in spinocerebellar ataxia type 1. Hum Mol Genet. 2018;27(16):2863-2873.
74. Dolan BM, Duron SG, Campbell DA, et al. Rescue of fragile X syndrome phenotypes in Fmr1 KO mice by the small-molecule PAK inhibitor FRAX486. Proc Natl Acad Sci U S A. 2013;110(14):5671-5676.
75. Civiero L, Cirnaru MD, Beilina A, et al. Leucine-rich repeat kinase 2 interacts with p21-activated kinase 6 to control neurite complexity in mammalian brain. J Neurochem. 2015;135(6):1242-1256.
76. Tudor EL, Perkinton MS, Schmidt A, et al. ALS2/Alsin regulates Rac-PAK signaling and neurite outgrowth. J Biol Chem. 2005;280(41):34735-34740.
77. Hadano S, Hand CK, Osuga H, et al. A gene encoding a putative GTPase regulator is mutated in familial amyotrophic lateral sclerosis 2. Nat Genet. 2001;29(2):166-173.

Figures

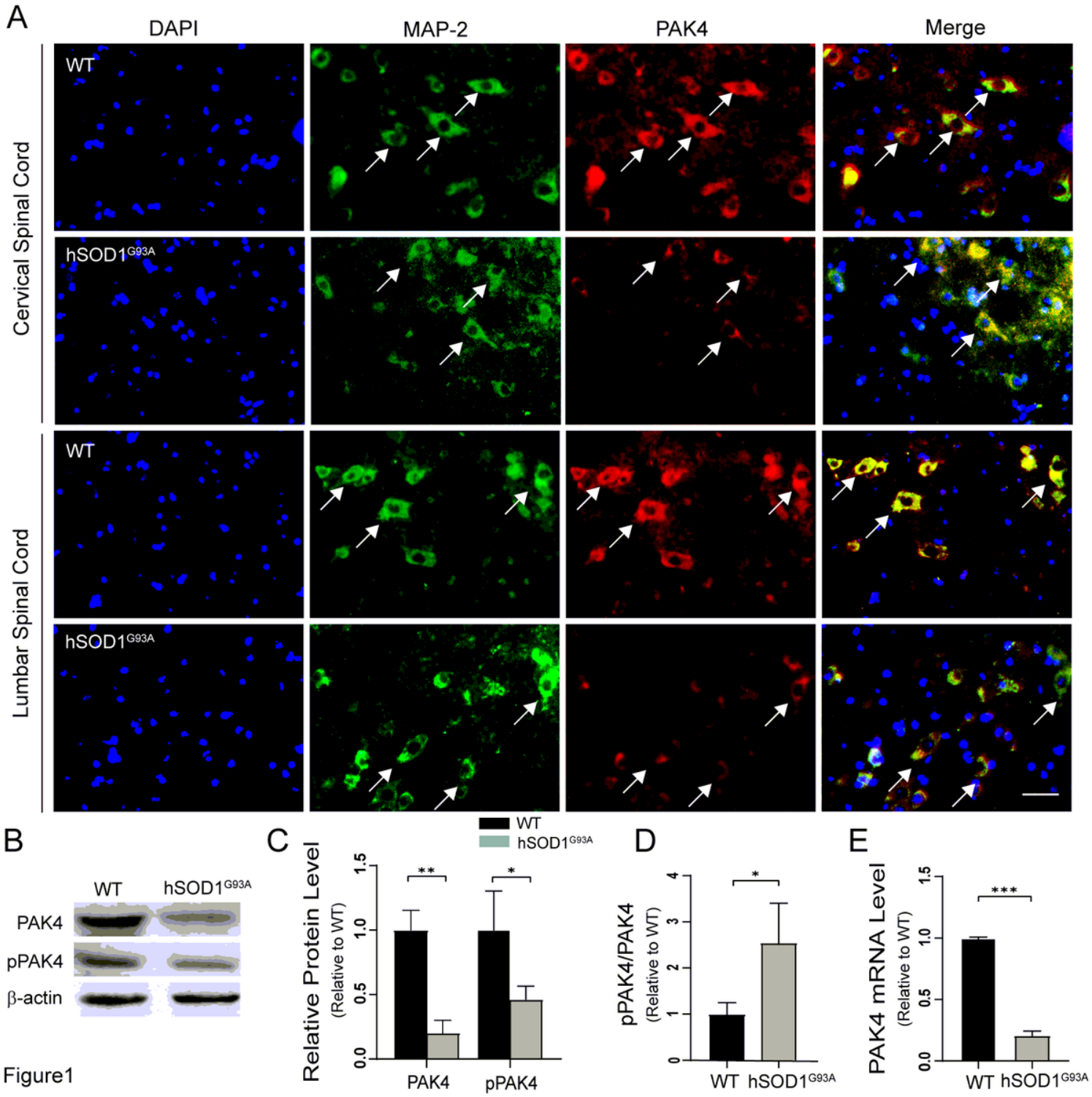

Figure1

Figure 1

Decreased PAK4 expression and activity in motor neuron of hSOD1G93A mice. (A) Confocal microscopy images showed that PAK4 expression in MN of p140 hSOD1G93A mice was lower than that of age-matched non-transgenic littermates (WT), n = 3/group. Scale bar =50 μm. (B) Immunoblotting of spinal cord extract from p140 hSOD1G93A mice and WT was conducted to detect PAK4 and pPAK4 expression. (C) Quantification of PAK4 and pPAK4 blots in (B) normalized to β-actin. Relative PAK4 and pPAK4 protein levels in hSOD1G93A mice were significantly downregulated. (D) pPAK4/PAK4 ratio in spinal

cords of hSOD1G93A mice was high. (E) qRT-PCR revealed that hSOD1G93A mice showed remarkably decreased PAK4 mRNA levels (n=6/group). Data were shown as means ± SD. Student's t test was used to evaluate statistical significance, *P < 0.05, **P < 0.01, ***p<0.001.

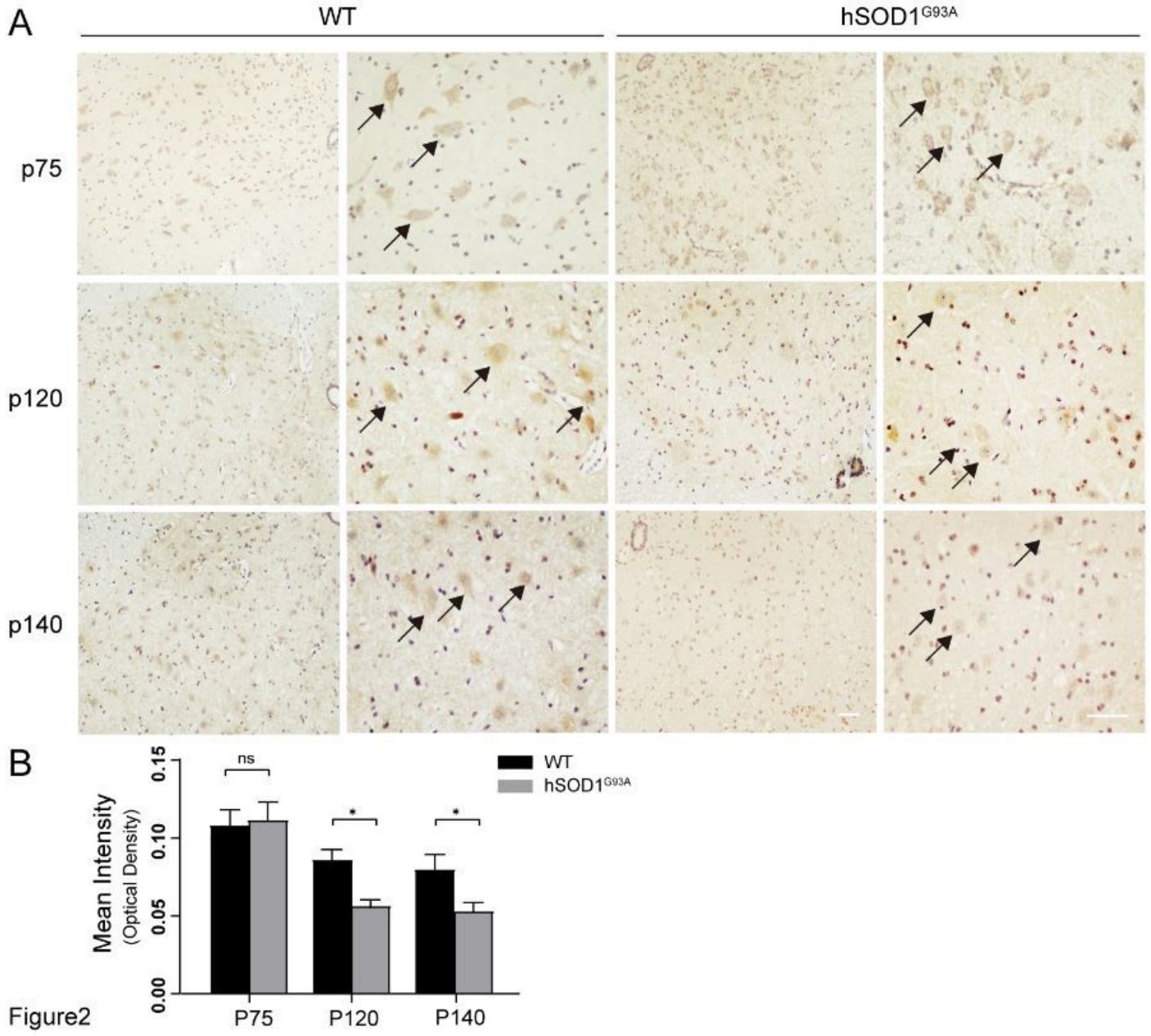

Figure 2

The intensity of PAK4 immunohistochemistry staining is decreased in motor neuron of hSOD1G93A mice at early-sym and late-sym stages. Paraffin sections of cervical spinal cords from hSOD1G93A mice and WT at three stages of the disease were subjected to immunohistochemistry. (A) PAK4-stained MNs (black arrow) were detected in the anterior horn of spinal cords from both hSOD1G93A mice and WT. Scale bar = 50 μm. (B) At stages p120 and p140, optical density (OD) values of PAK4 significantly decreased in hSOD1G93A mice, while there was no deregulation at stages p75 (n = 3/group, 6 sections/mouse). Data were provided as means ± SD and were tested for significance using Student's t test. ns ≥ 0.05, *p < 0.05.

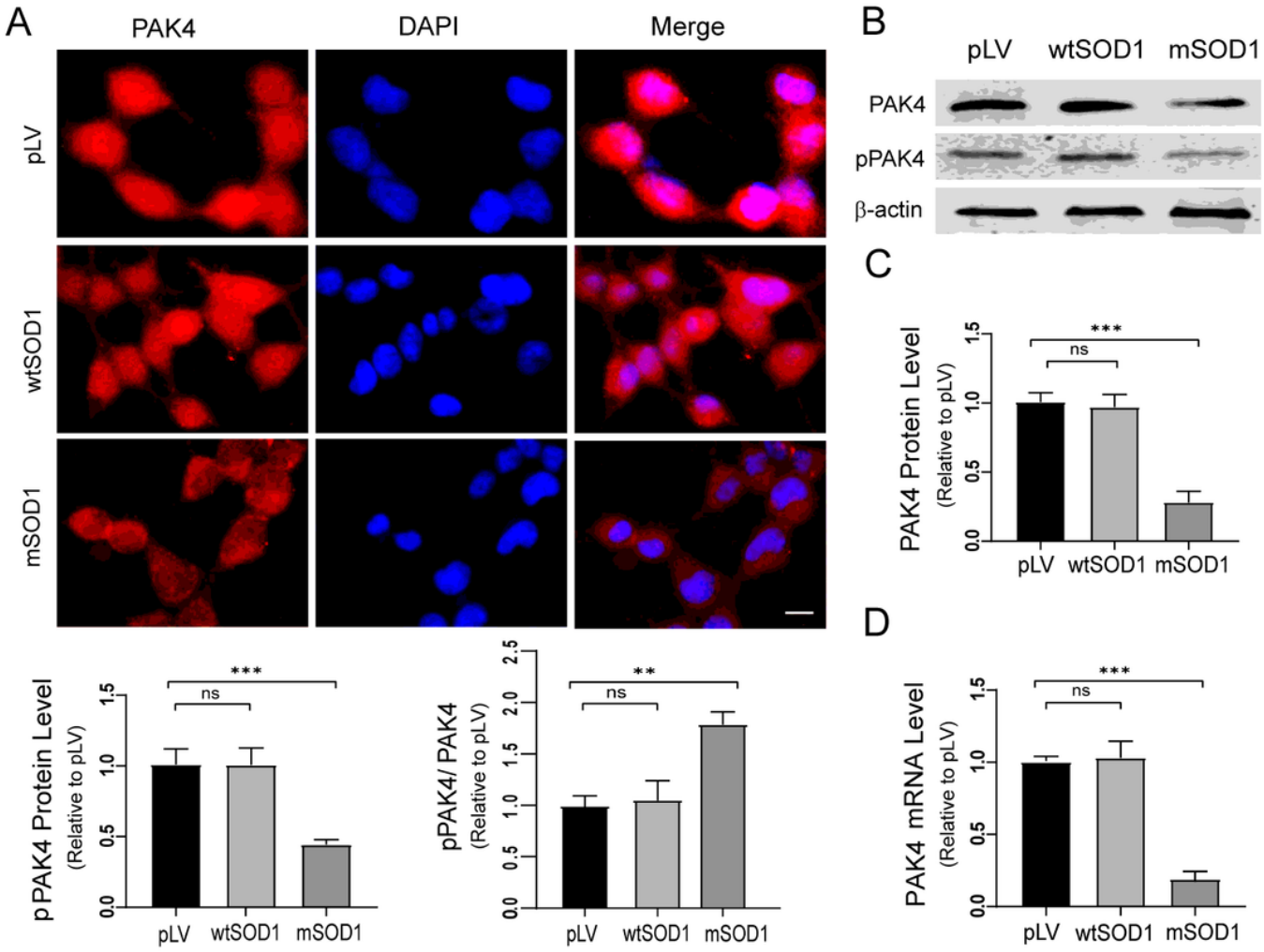

Figure3

Figure 3

Reduced expression of PAK4 is identified in mSOD1 cells. NSC34 cells were stably transfected with human wild-type SOD1 (wtSOD1), mutant SOD1 (mSOD1) or empty lentivirus vector (pLV). (A) Confocal microscopy images of PAK4 (red) in pLV, wtSOD1 and mSOD1 cells, respectively. The weakest intensity of PAK4 staining was observed in mSOD1 cells, while similar intensities were seen in wtSOD1 and pLV cells. Scale bar = 50 μm. (B) Immunoblotting analysis of PAK4 and pPAK4 protein expression levels was conducted with lysates from control pLV, wtSOD1 and mSOD1 cells. (C) Quantification of PAK4 and pPAK4 blots in (B) normalized to β-actin. Relative PAK4 and pPAK4 protein levels were significantly decreased in mSOD1 cells. pPAK4/PAK4 ratio was highest in mSOD1 cells. (D) qRT-PCR analysis detected the mRNA expression of PAK4. For relative quantification of PAK4 mRNA expression, the 2−ΔΔCt method was conducted using β-actin for normalization; data were provided as means ± SD. ANOVA with Student-Newman-Keuls post hoc analysis was used to evaluate statistical significance, ns≥0.05, *p<0.05 , **p<0.01, ***p<0.001.

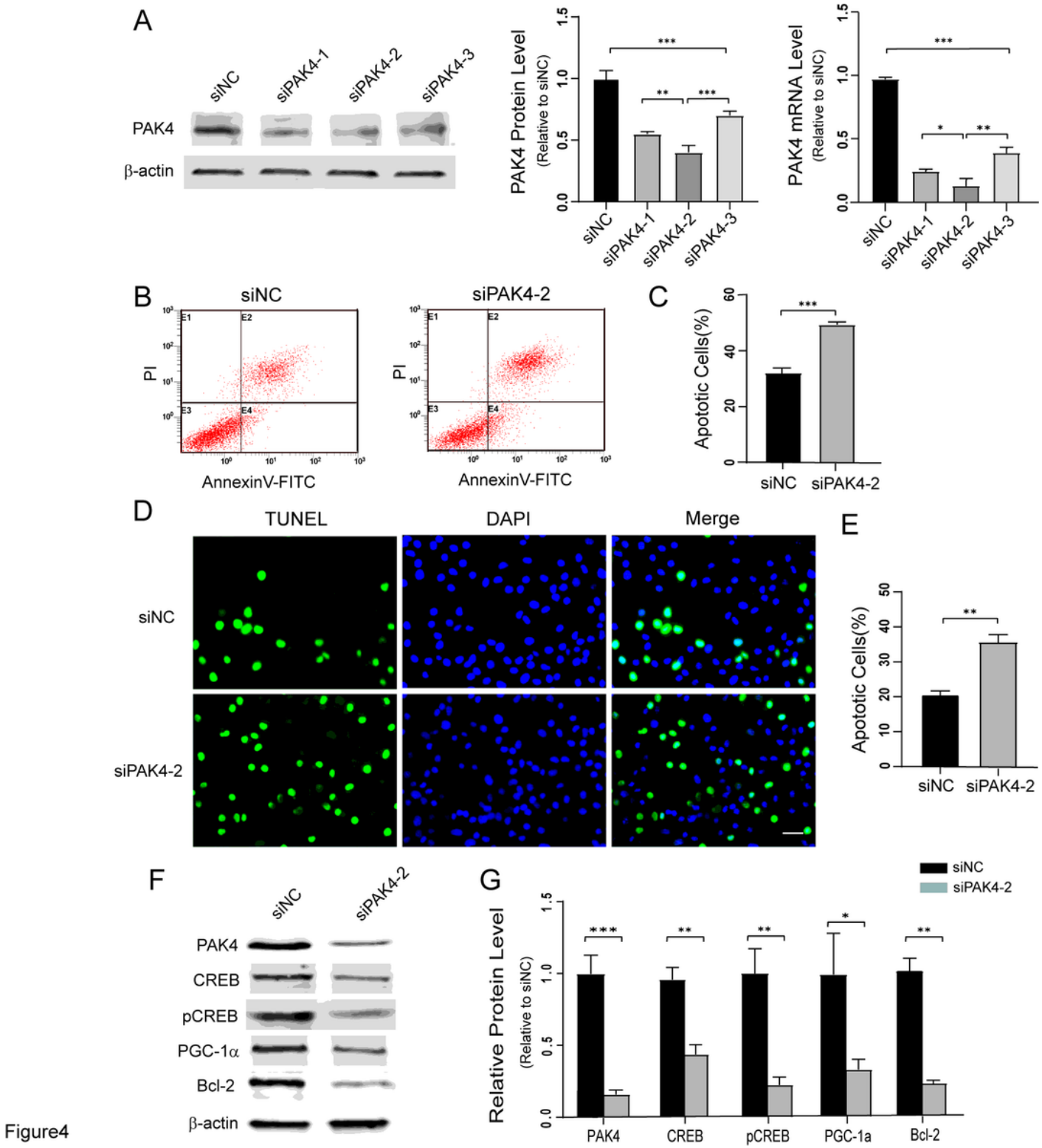

Figure4

Figure 4

Knockdown of PAK4 triggers neurodegeneration and inhibits CREB pathway. (A) Western blotting analysis of the efficiency of PAK4 knockdown using siRNAs. The mRNA level of PAK4 was detected by qRT-PCR in NSC34 cells transfected with siNC or siPAK4. (B) Flow cytometry detected the apoptosis of NSC34 cells after transfection with siPAK4-2 or siNC for 72 h. (C) Quantification of cell apoptosis. (D and E) TUNEL staining of NSC34 cells after treatment with siPAK4-2. (F) Western blotting of PAK4/CREB pathway

signaling proteins expression levels in PAK4 knockdown NSC34 cells. (G) Quantification of the blots in (F) normalized to β-actin. Data were presented as means ± SD. *P < 0.05, **P < 0.01, ***p<0.001. Student's t test (C, E, G) or ANOVA with Student- Newman-Keuls post hoc analysis (A). Scale bar = 50 μm.

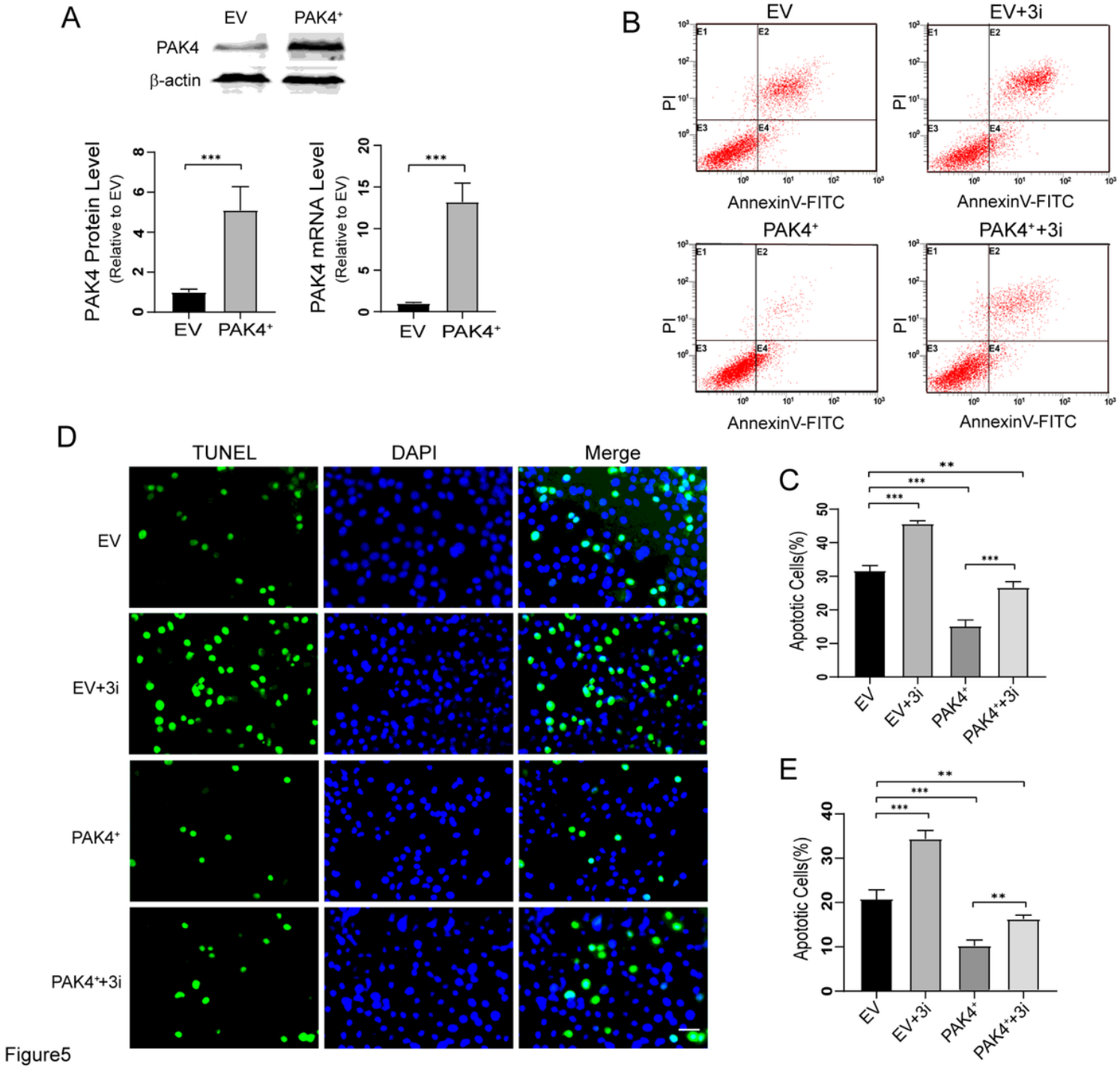

Figure5

Figure 5

Overexpression of PAK4 protects mSOD1 cells from degeneration. (A) Western blotting and qRT-PCR analysis of mSOD1 cells transfected with PAK4 plasmid or EV, and β-actin served as a loading control. (B and C) 48 h after transfection, mSOD1 cells were incubated with 3i (50.26 ng/ml), and cell apoptosis was determined by flow cytometry. (D) The mSOD1 cells transfected with PAK4 plasmid or EV were treated

with 3i (50.26 ng/ml) for 72 h. Then, cell apoptosis was determined by TUNEL staining. Scale bar = 50 μm. (E) Quantification of the TUNEL staining. Data from the experiments were presented as means ± SD. *P < 0.05, **P < 0.01, ***p<0.001, vs. Control group. ANOVA with Student-Newman- Keuls post hoc analysis (C, E) or Student's t test (A).

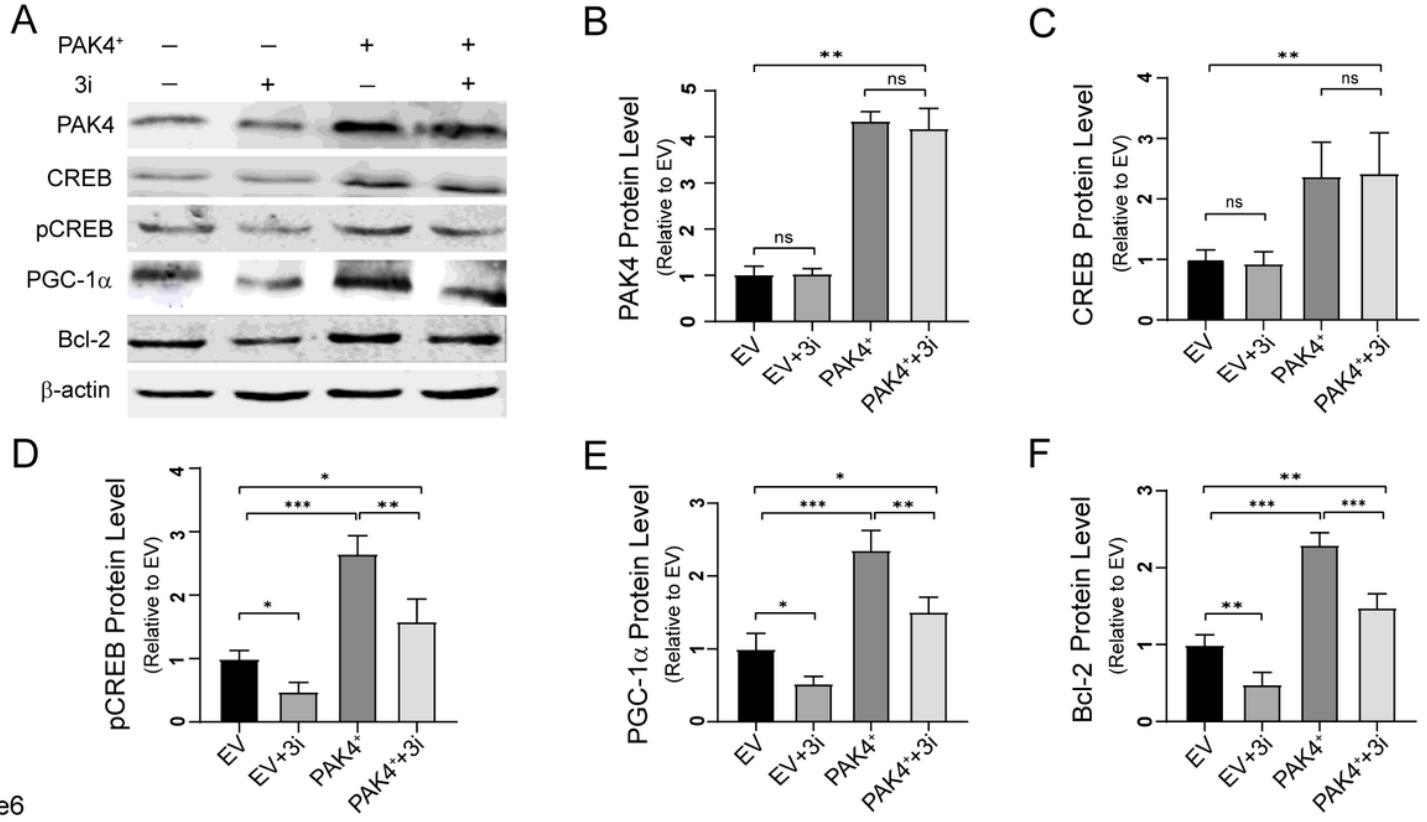

Figure6

Figure 6

CREB pathway mediates PAK4-induced neuroprotection. (A) Immunoblotting of cell extract from EV, EV+3i, PAK4+ and PAK4++3i groups. (B-F) Quantitative analysis of PAK4 (B), CREB (C), pCREB (D), PGC-1a (E), and Bcl-2 (F) levels in (A) normalized to β-actin. Data were presented as means ± SD. ns ≥ 0.05, *P < 0.05, **P < 0.01, ***p<0.001, vs. Control group. ANOVA with Student-Newman-Keuls post hoc analysis.

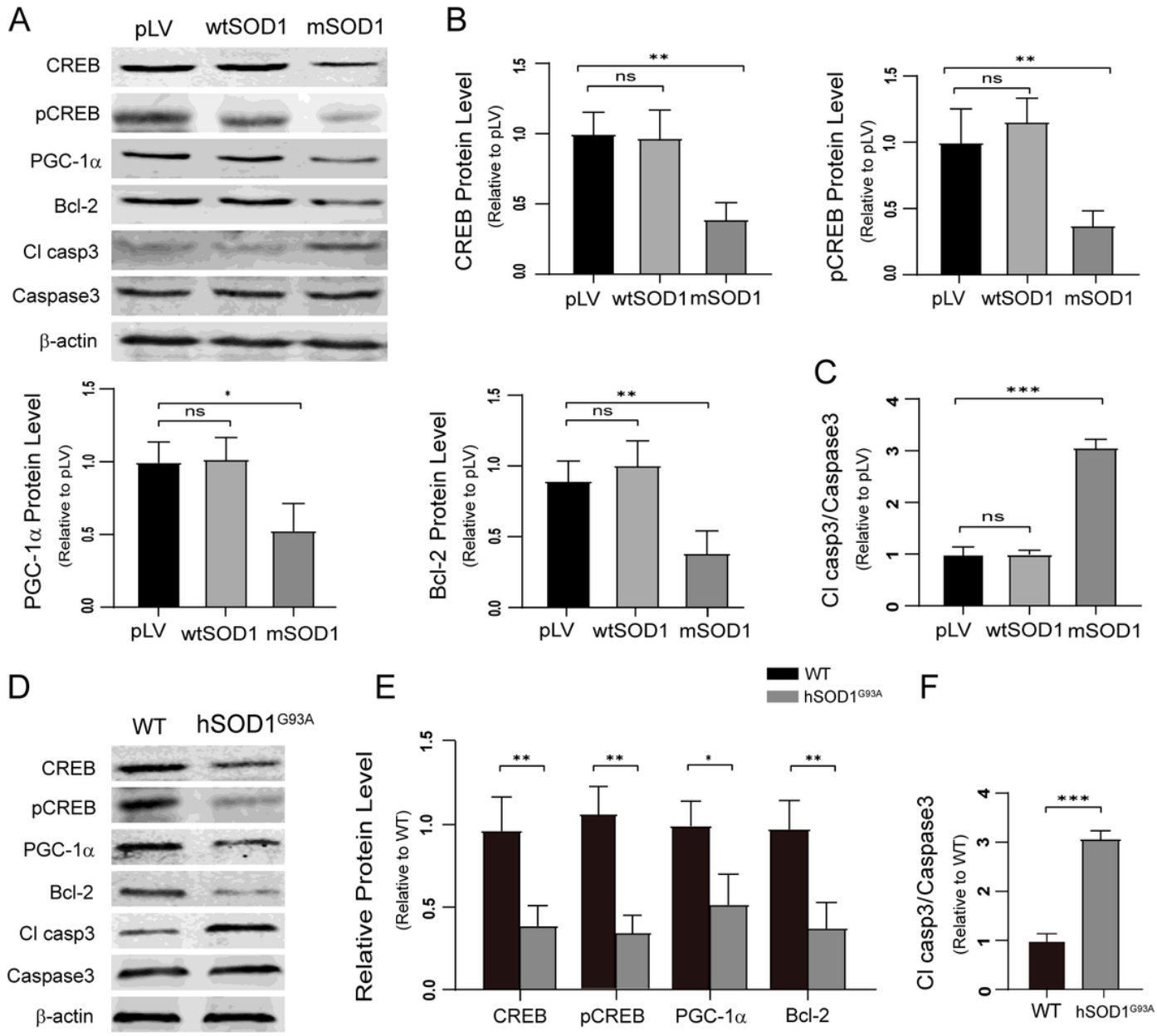

Figure7

Figure 7

CREB signaling is deregulated and motor neuron degeneration is increased in ALS in vitro and in vivo models. (A) Western blotting analysis of CREB, pCREB, PGC-1a, Bcl-2, caspase3 and cleaved-caspase3 levels was conducted with samples from pLV and mSOD1 cells. (B) Quantification analysis of CREB, pCREB, PGC-1a and Bcl-2 normalized to β-actin. (C) Quantification analysis of cleaved-caspase3 normalized to caspase3. (D) CREB, pCREB, PGC-1a, Bcl-2, caspase3 and cleaved-caspase3 levels of the spinal cord lysates from WT and hSOD1G93A mice. (E) Quantification of CREB, pCREB, PGC-1a and Bcl-2 normalized to β-actin. (F) Quantification analysis of cleaved-caspase3 normalized to caspase3. Data were presented as means ± SD. ns ≥ 0.05, *P < 0.05, **P < 0.01, ***p<0.001 vs. Control group. Student's t test.

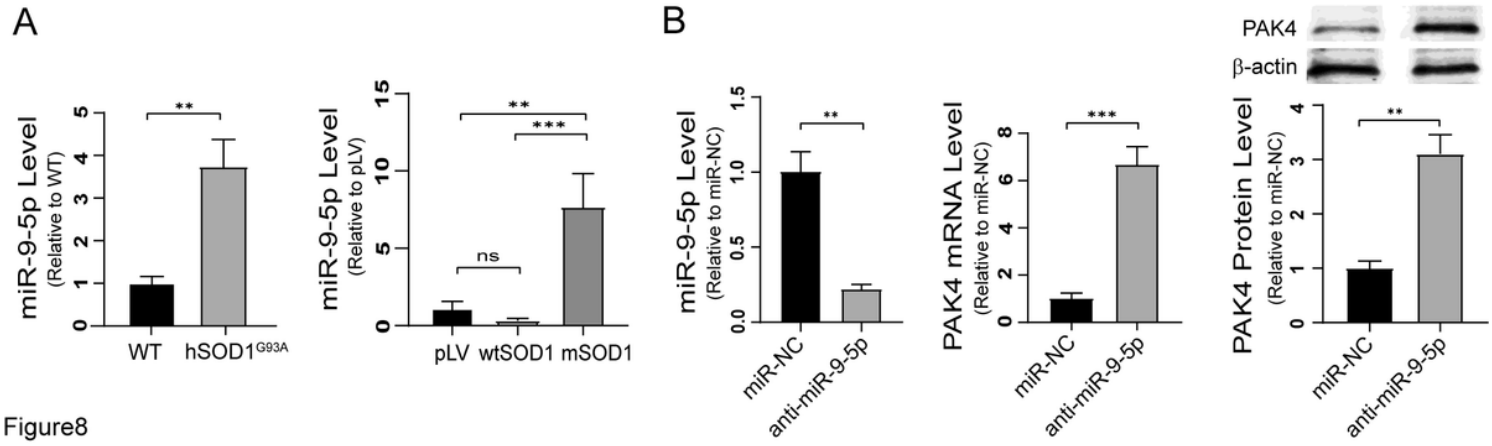

Figure8

Figure 8

miR-9-5p is upregulated and inversely regulates PAK4 mRNA expression in ALS. (A) The expression of miR-9-5p in spinal cords from hSOD1G93A mice and in mSOD1 cells was determined by qRT-PCR. (B) The expression of miR-9-5p and PAK4 at mRNA and protein levels in mSOD1 cells transfected with anti-miR-9-5p or miR-NC were determined by qRT-PCR and western blotting. Data were presented as means ± SD. *P < 0.05, **P < 0.01, ***p<0.001 vs. Control group. Student's t test.

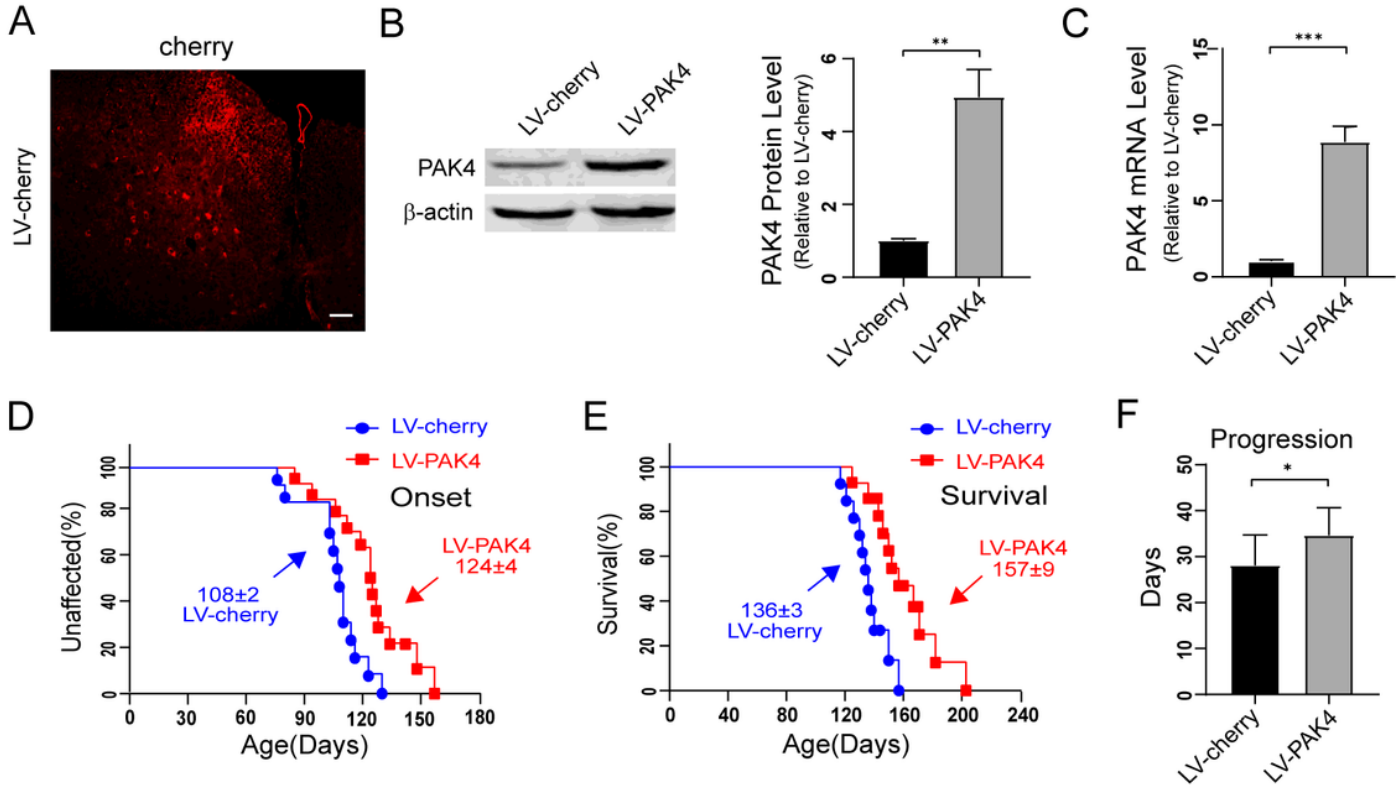

Figure9

Figure 9

Overexpression of PAK4 in the spinal cord delays disease onset and increases the lifespan of hSOD1G93A mice. (A) The spinal cord sections of hSOD1G93A mice injected with LV-cherry (red) were examined for cherry expression. Scale bar = 50 μm. (B) Western blotting was performed to determine the

long-lasting effects and efficiency of LV-PAK4 expression. (C) RNA collected from the spinal cords of LV-PAK4/LV-cherry injected hSOD1G93A mice was used to analyze PAK4 mRNA levels by qRT-PCR. (D-F) LV-PAK4 intraspinal injection into p60 hSOD1G93A mice significantly postponed median disease onset (D) compared with LV-cherry (LV-PAK4:124 d; LV-cherry:108 d; $P < 0.01$) and extended median survival (E) (LV-PAK4: 157 d; LV-cherry: 136 d; $P < 0.01$) and disease progression (F) (LV-cherry: 28 d; LV-PAK4: 35 d; $P < 0.05$). Data represent means ± SD. Statistical analyses were performed using Student's t test or Kaplan-Meier survival analysis. *p < 0.05, **p < 0.01, ***p<0.001.

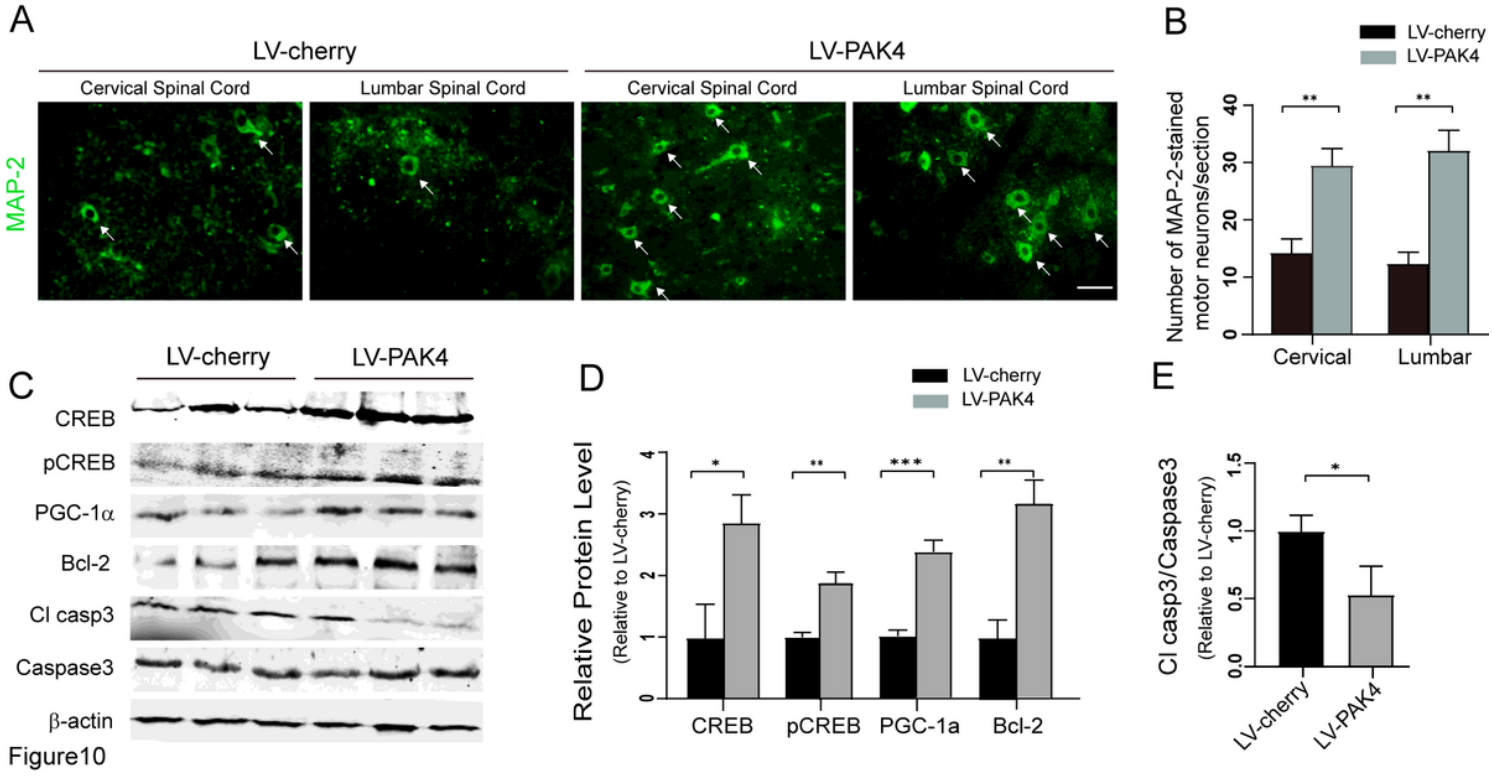

Figure 10

Overexpression of PAK4 in the spinal cord suppresses motor neuron degeneration and increases the activity of the CREB signaling pathway in hSOD1G93A mice. (A) Immunostaining of MAP-2 in the ventral horn (VH) of the spinal cords from LV-cherry/LV-PAK4 injected hSOD1G93A mice at P135. (B) Number of MAP-2-stained MNs in the VH of LV-cherry/LV-PAK4 treated hSOD1G93A mice. Scale bar = 50 μm. (C) CREB, pCREB, PGC-1a, Bcl-2, caspase3 and cleaved-caspase3 levels of the spinal cord from LV-cherry/LV-PAK4 injected hSOD1G93A mice. (D) Quantification of CREB, pCREB, PGC-1a and Bcl-2 normalized to β-actin. (E) Quantification analysis of cleaved-caspase3 normalized to caspase3. Data represent means ± SD, n = 3/group. Statistical analyses were performed using Student's t test .*p < 0.05, **p < 0.01, ***p<0.001.

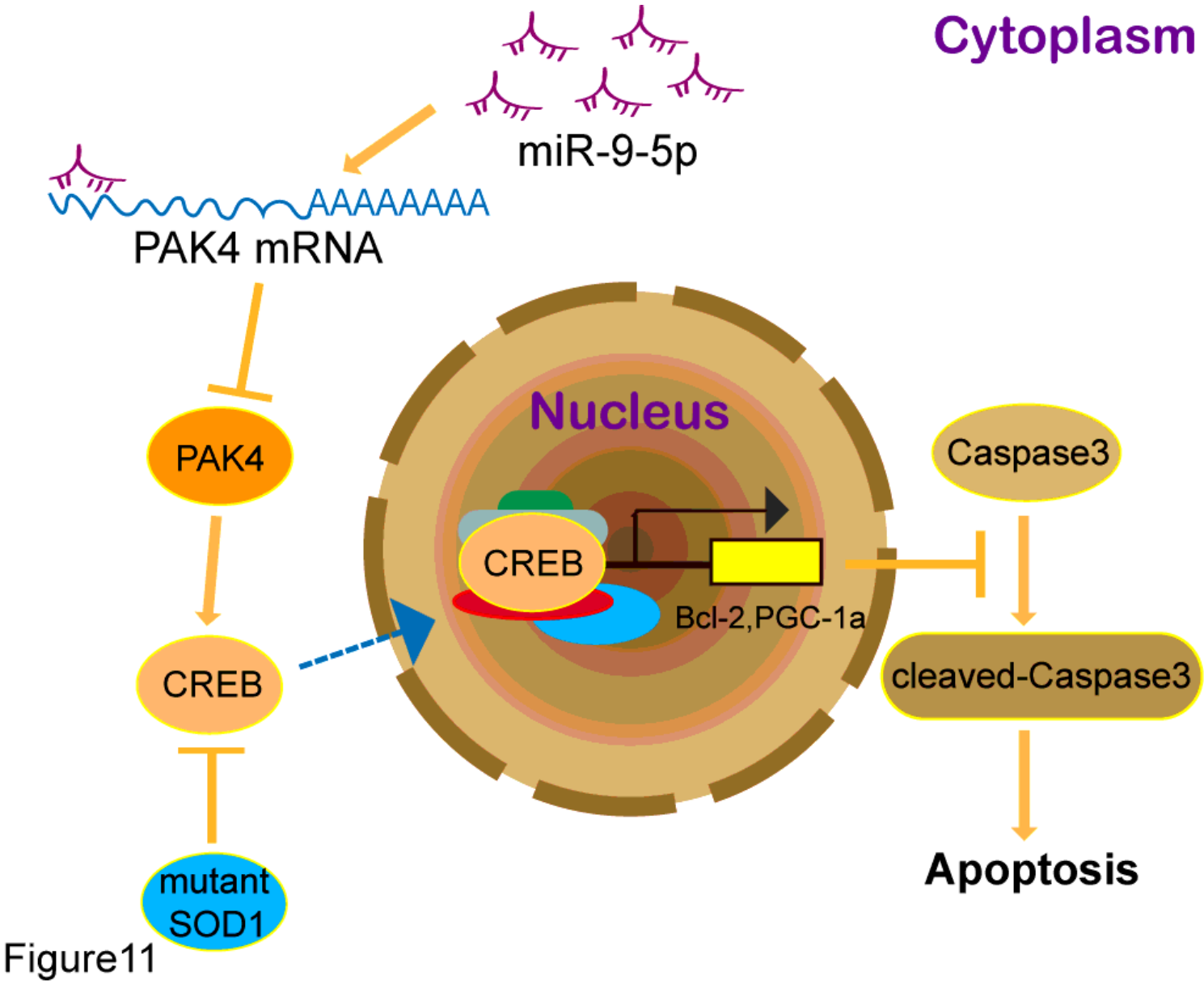

Figure 11

Schematic representation of the neuroprotective role of PAK4 in ALS. PAK4 increases CREB levels and activity, leading to the upregulation of PGC-1a and Bcl-2, thereby decreasing cleaved-caspase3 levels, and inhibiting motor neuron degeneration. miR-9-5p is responsible for the decreased expression of PAK4 in ALS.